Simulation of reactive PA6 flow in a fibrous preform for T-RTM process

International conference on composite materials | Belfast 2023

William Han[1,2], Quentin Govignon[2], Arthur Cantarel[2], Fabrice Schmidt[2]

[1] Mines Paris, Université PSL, Centre des Matériaux (MAT), France

[2] Institut Clément Ader (ICA), Université de Toulouse, CNRS, IMT Mines Albi, INSA, ISAE-SUPAERO, UPS, France,

31st July 2023

Thermoplastics composites

Composite materials

- Combine specific properties of materials
- Popular alternative to metal alloys
  - Lower weight

Thermoplastics

- Re-workable
- Repairable
- “Recyclable”
- Good mechanical properties

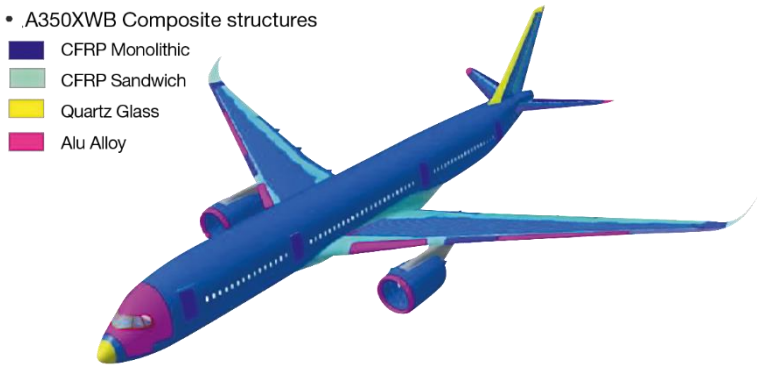

A350 XWB Composite Structures
safetyfirst.airbus.com

BMW i3, electric car with thermoplastic skin
plastix-world.com

RTM processing of thermoplastics (TP-RTM)

RTM Process *(Resin Transfer Moulding):*

- Composite with complex shapes
- High production rates
- Moderate costs
- Control fibrous preform properties

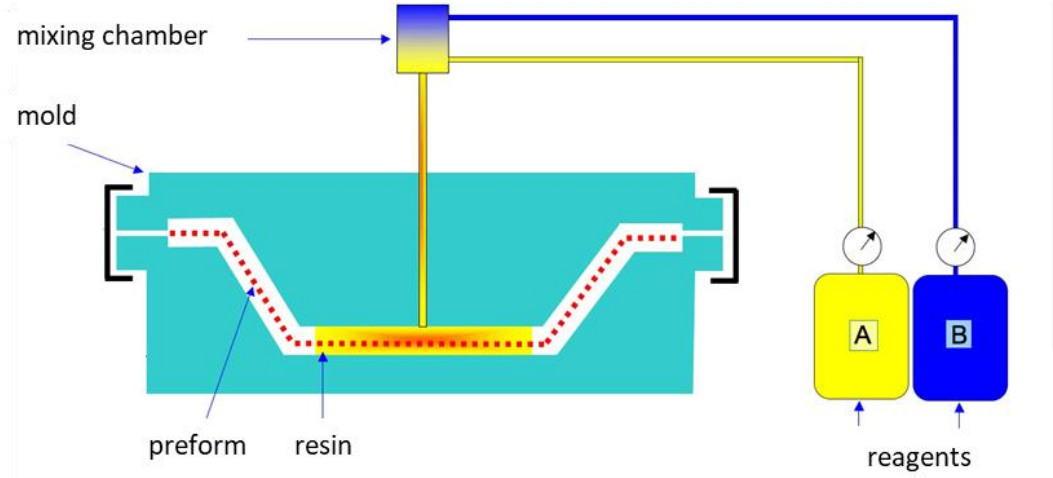

Materials

- **Low viscosity resin**
- Fibrous preform

Thermoplastics melts

- High viscosity
- High temperature

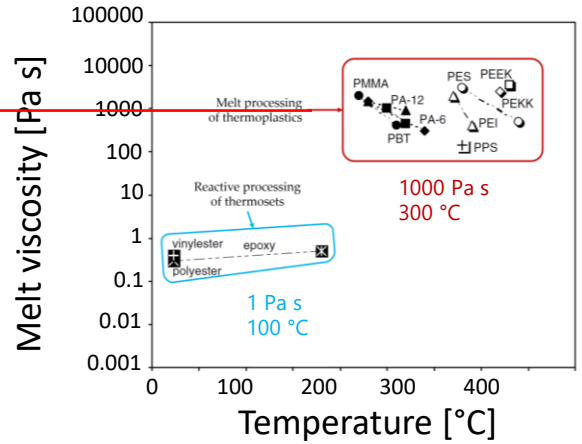

van Rijswijk et al. (2007)

RTM processing of thermoplastics (TP-RTM)

RTM Process *(Resin Transfer Moulding):*

- Composite with complex shapes
- High production rates
- Moderate costs
- Control fibrous preform properties

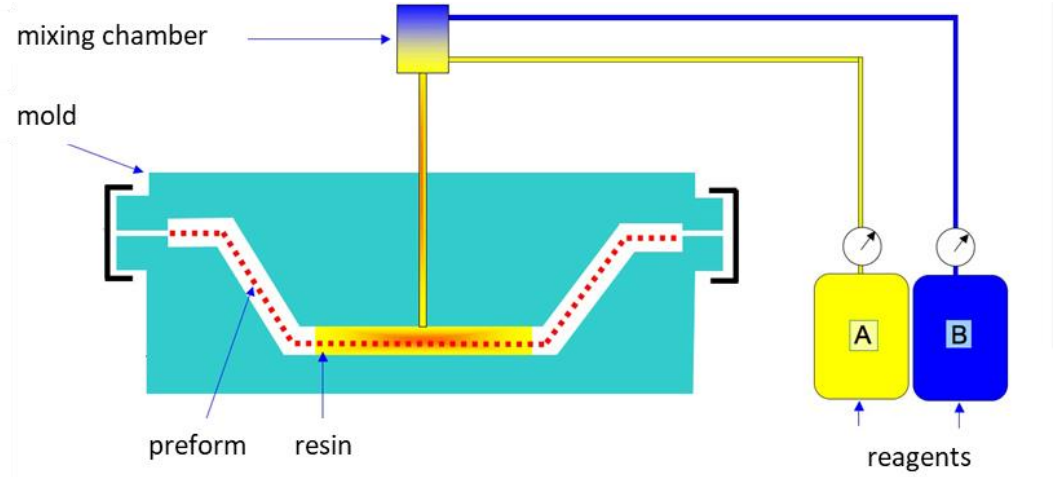

Materials

- **Low viscosity resin**
- Fibrous preform

Reactive thermoplastic

+ Low viscosity
+ Moderate temperature

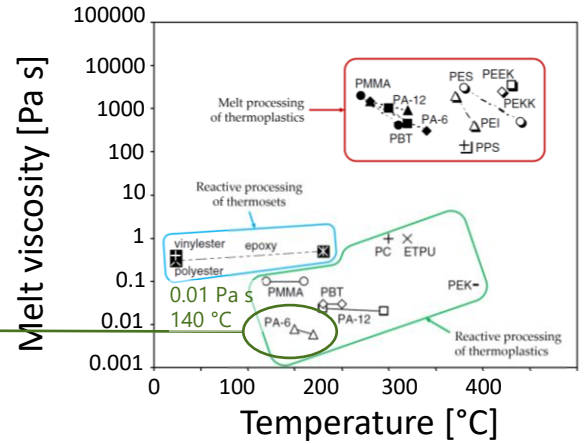

van Rijswijk et al. (2007)

Reactive mix for anionic synthesis of PA6

Reactants

Catalyst (MgBrCL)

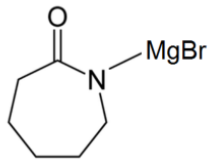

7.73% mass fraction

monomer (ε-caprolactam)

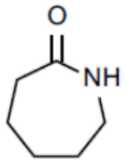

84.55% mass fraction

Activator (HDCL)

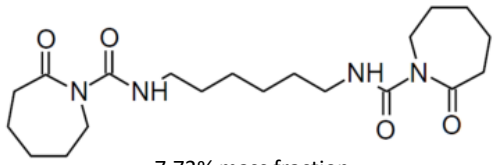

7.73% mass fraction

Product

Polyamide 6 (PA6)

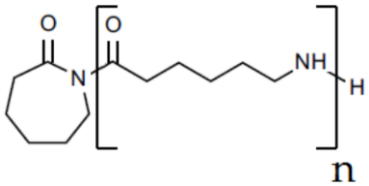

Synthesis characterization

DSC isothermal syntheses

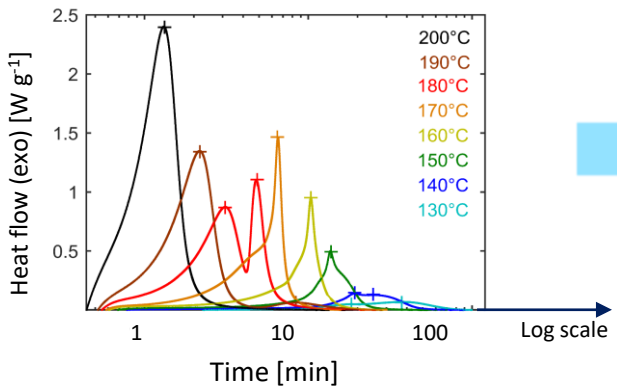

Synthesis model

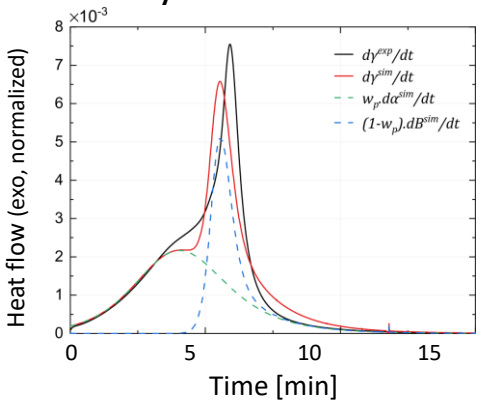

TTT Diagram

(Time Temperature Transformation)

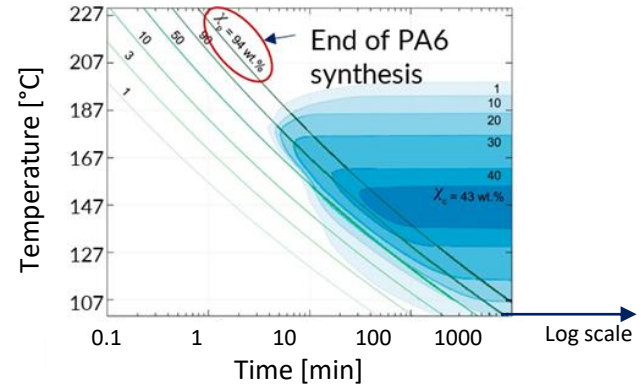

C. Vicard, O. De Almeida, A. Cantarel, and G. Bernhart. (2017, 2019)
C. Vicard (2018), Institut Clément Ader

Resin flow in a fibrous preform

INSTITUT CLÉMENT ADER

Continuous fibre preform

- Gaps between tows
- Gaps between fibres

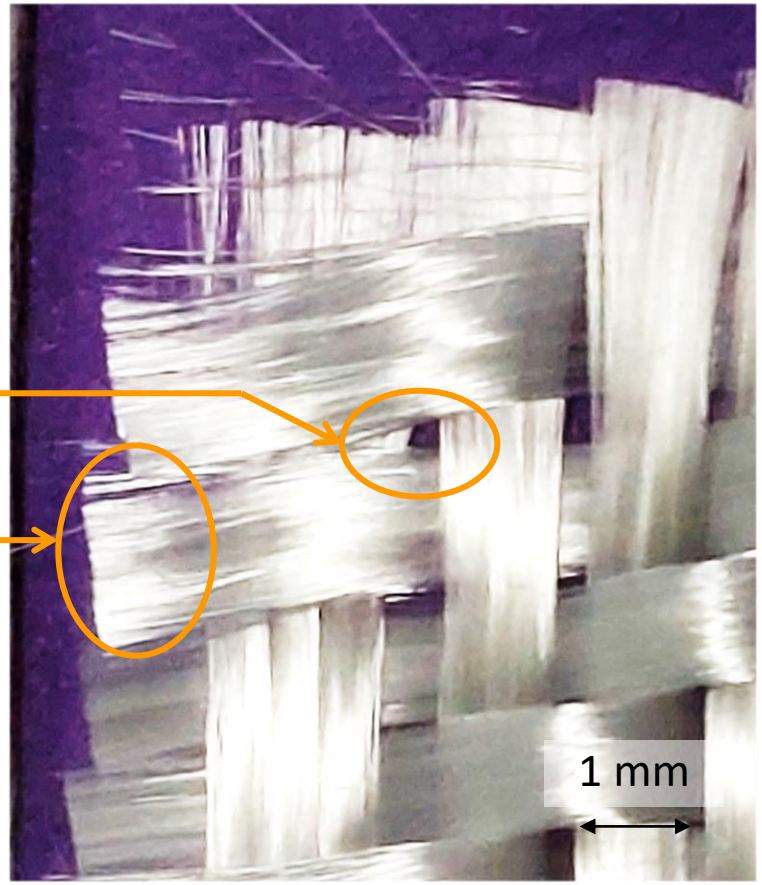

Dual scale porosity in continuous fibre preforms

Resin flow in a fibrous preform

Dual scale flow

- Intra-tow
  - Between fibres
- Inter-tow
  - Between tows

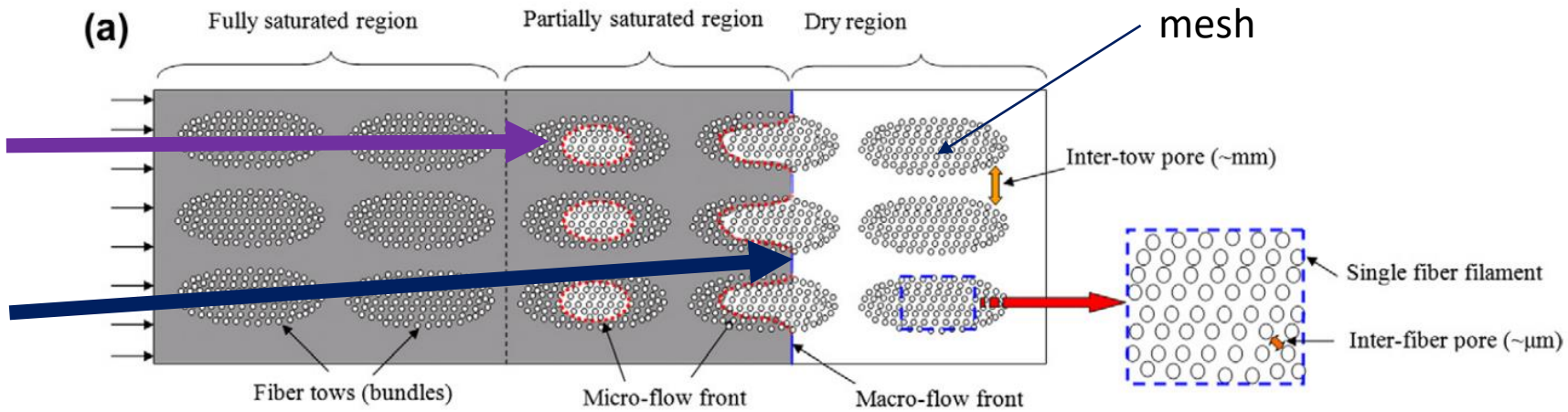

H. Tan et K.M. Pillai (2012)

Resin flow in a fibrous preform

Dual scale flow

- Intra-tow
  - Between fibres
- Inter-tow
  - Between tows

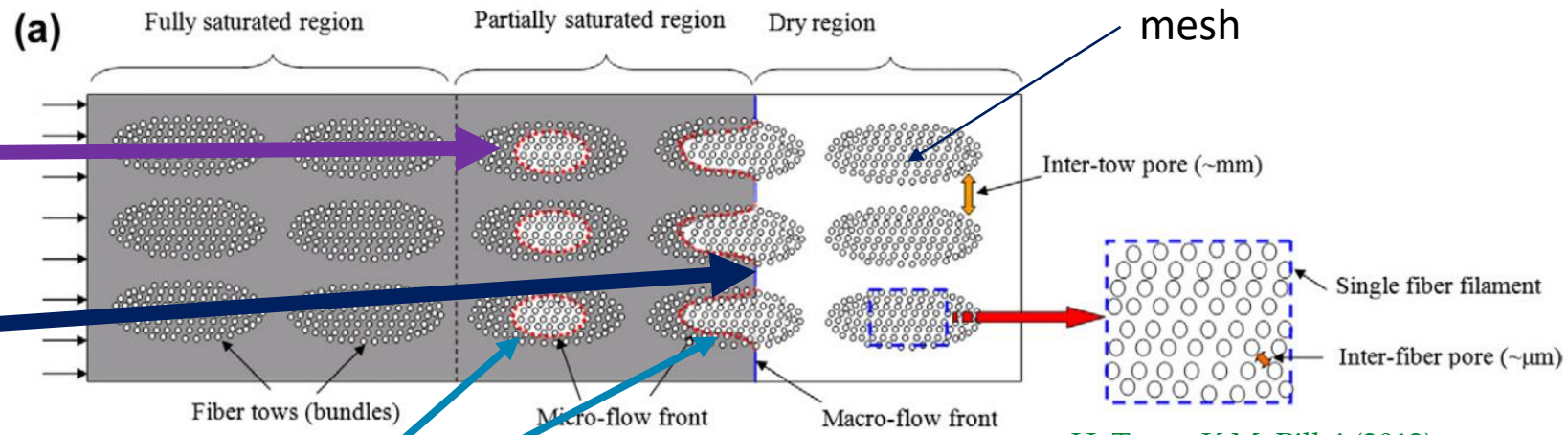

H. Tan et K.M. Pillai (2012)

- Fast flow between tows (non-wetting resins)
- Slow impregnation inside tows
- Resin release from tows

M. Imbert et al. (2017)

Resin ages differently inside tows and between tows

Resin flow in a fibrous preform

Dual scale flow

- Intra-tow
  - Between fibres
- Inter-tow
  - Between tows

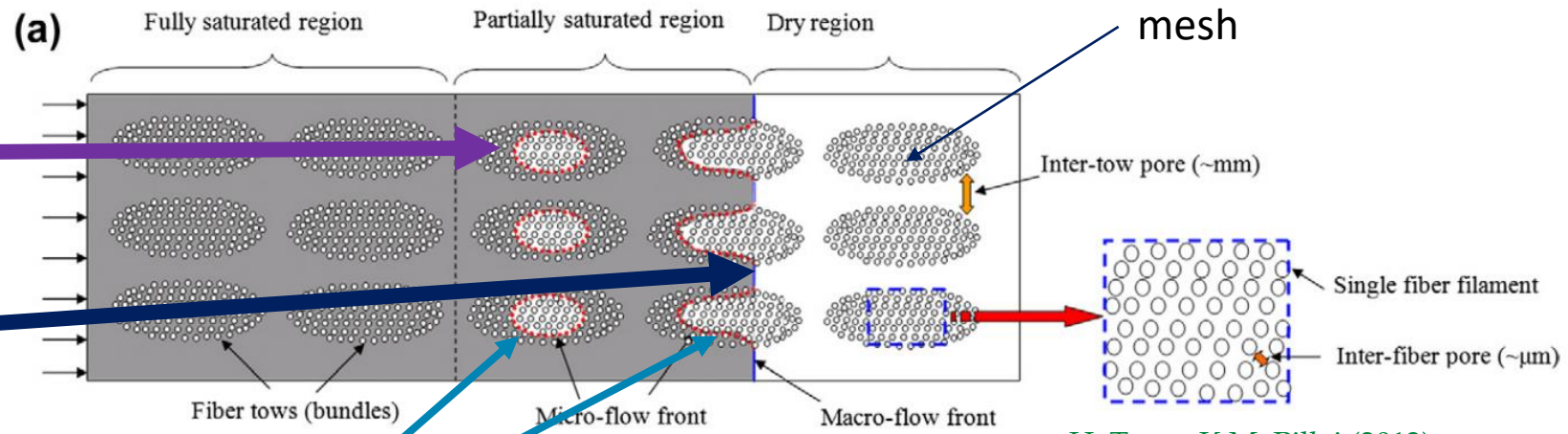

H. Tan et K.M. Pillai (2012)

- Fast flow between tows (non-wetting resins)
- Slow impregnation inside tows
- Resin release from tows

M. Imbert et al. (2017)

Resin ages differently inside tows and between tows

Impact on composite

- Gas bubbles formation and transport
- Non-homogeneous synthesis
- Effect of synthesis shrinkage

Injection simulation principle

Simulations using OpenFOAM ® 8.x

- **Open source CFD toolbox**

- **Finite Volume method (FVM)**
  - Discretization of the transport equation of a field ϕ in a finite volume using Gauss's theorem

$$\int_{V_p} \frac{\partial \rho \phi}{\partial t} dV + \int_{V_p} \boldsymbol{\nabla} \cdot (\rho \phi \boldsymbol{u}) dV - \int_{V_p} \boldsymbol{\nabla} \cdot (\rho \Gamma \boldsymbol{\nabla} \phi) dV = \int_{V_p} S_\phi dV$$

- **PISO method for incompressible Navier-Stokes resolution**

$$\nabla \cdot \boldsymbol{u} = 0$$ Continuity equation

$$\rho \left[\frac{\partial \boldsymbol{u}}{\partial t} + \boldsymbol{\nabla} \cdot (\rho \boldsymbol{u} \otimes \boldsymbol{u}) \right] = -\nabla p + \eta \boldsymbol{\Delta u}$$ Momentum equation

- **Ubuntu 18.04.06 virtual machine specifications**

Memory	31,4 GiB
Processor	AMD® Ryzen threadripper 3960x 24-core processor × 8

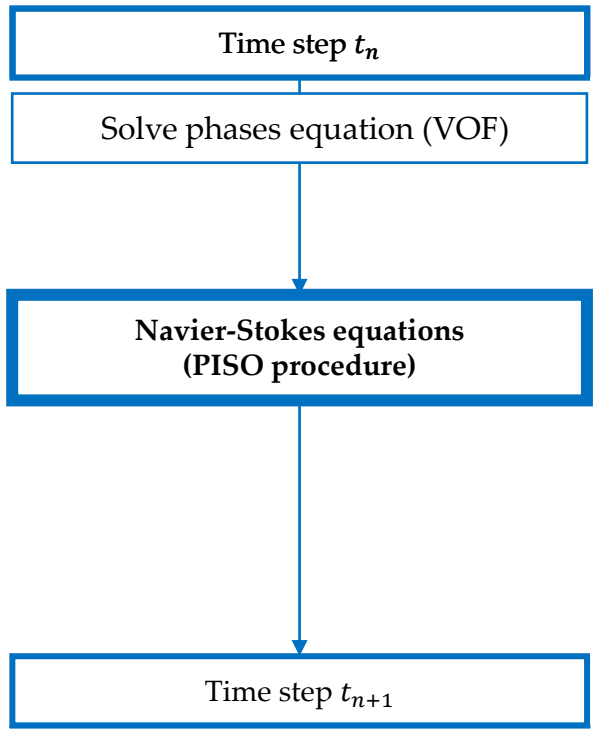

Injection simulation principle

Simulations using OpenFOAM ® 8.x

- **Open source CFD toolbox**
- **Finite Volume method (FVM)**
  - Discretization of the transport equation of a field ϕ in a finite volume using Gauss's theorem

$$\int_{V_p} \frac{\partial \rho\phi}{\partial t} dV + \int_{V_p} \boldsymbol{\nabla} \cdot (\rho\phi\boldsymbol{u}) dV - \int_{V_p} \boldsymbol{\nabla} \cdot (\rho\Gamma\boldsymbol{\nabla}\phi) dV = \int_{V_p} S_\phi dV$$

- **PISO method for incompressible Navier-Stokes resolution**

$$\nabla \cdot \boldsymbol{u} = 0$$ Continuity equation

$$\rho\left[\frac{\partial \boldsymbol{u}}{\partial t} + \boldsymbol{\nabla} \cdot (\rho\boldsymbol{u}\otimes\boldsymbol{u})\right] = -\nabla p + \eta\boldsymbol{\Delta u}$$ Momentum equation

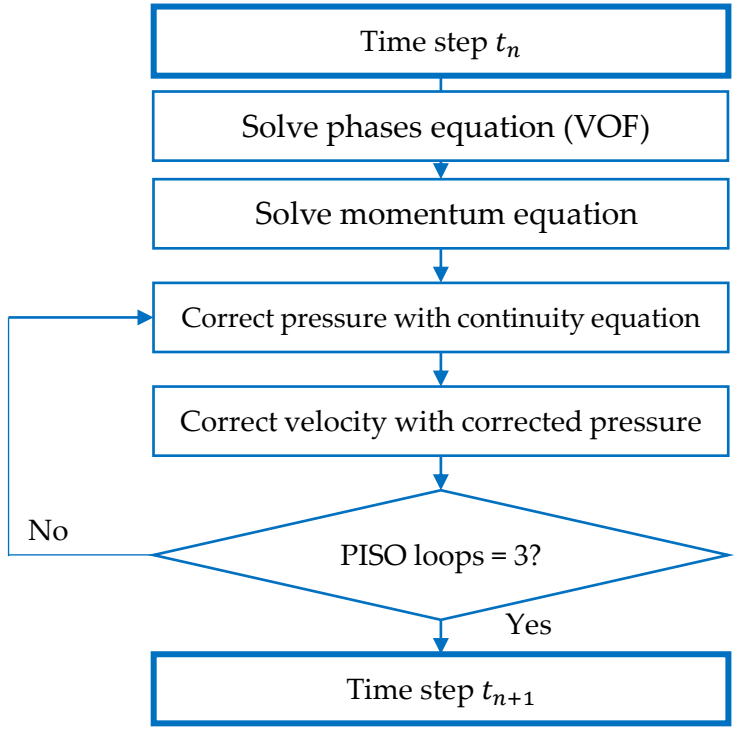

- **Ubuntu 18.04.06 virtual machine specifications**

Memory	31,4 GiB
Processor	AMD® Ryzen threadripper 3960x 24-core processor × 8

Flow simulation in fibrous preform

Navier-Stokes-Brinkman equation

$$\frac{\rho}{\tilde{\varepsilon}}\left[\frac{\partial \bar{\boldsymbol{u}}}{\partial t} + \nabla\left(\frac{\bar{\boldsymbol{u}}\cdot\bar{\boldsymbol{u}}}{\tilde{\varepsilon}}\right) - \nu\boldsymbol{\Delta}\bar{\boldsymbol{u}}\right] = -\nabla p + \eta\boldsymbol{K}^{-1}\bar{\boldsymbol{u}}$$

- $\bar{\boldsymbol{u}}$: averaged velocity vector
  - $\tilde{\varepsilon}$: porosity
- $\boldsymbol{K}$: permeability tensor
  - Flow hydraulic conductivity

$$\boldsymbol{u} = \frac{\bar{\boldsymbol{u}}}{\tilde{\varepsilon}}$$

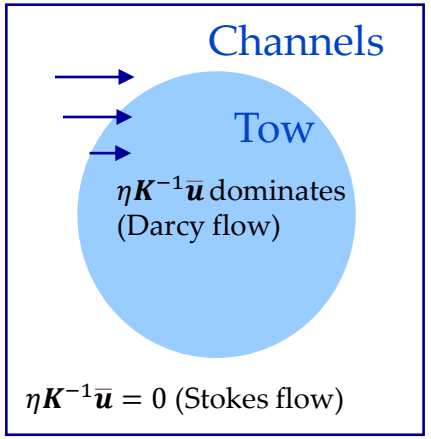

Handle flow both inside and between tows

Saturation equation

$$\frac{\partial \tilde{\varepsilon} S_1}{\partial t} + (\boldsymbol{\nabla}\cdot\bar{\boldsymbol{u}}_1)S_1 + \boldsymbol{\nabla}\cdot(\bar{\boldsymbol{u}}_1 - \bar{\boldsymbol{u}}_2)S_1 S_2) = 0$$

- VOF equation from Wardle et Weller (2013) is modified and becomes conservation of saturation S_1

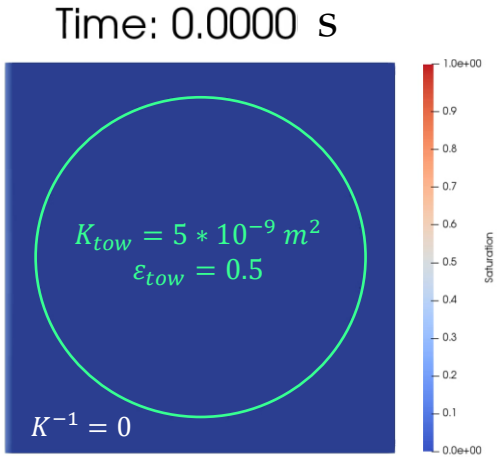

Realistic tow geometry

Digitization of a textile sample

- Realized in Wijaya PhD Thesis (2020)
  - µ-tomography of a woven sample

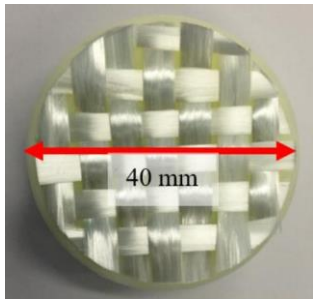

Textile sample

µCT scanner

Grayscale levels

Voxelization

Voxel meshing

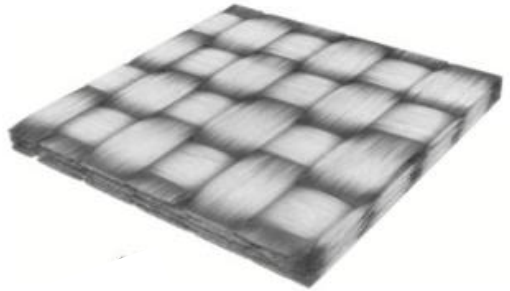

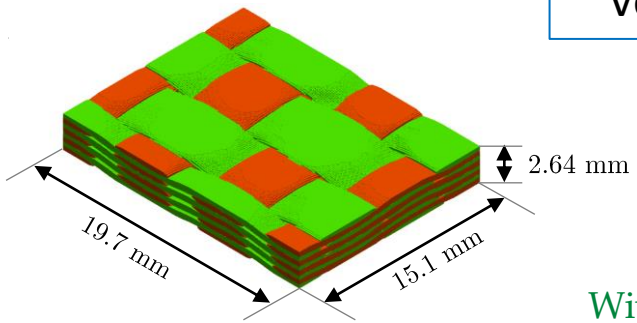

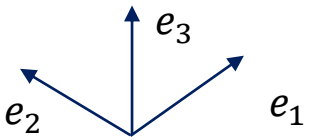

Wijaya (2020)

Tows permeability

- Permeability inside each tow voxel calculated with Gebart hypotheses

Wijaya (2020), University of Auckland (NZ)

- Averaged geometrically in tows of each direction

$$\log \bar{K} = \sum_{i=1}^{n} \log \frac{k_i}{n}$$

$$\bar{K}_{tows,weft} = \begin{bmatrix} 1.78 \cdot 10^{-12} & 0 & 0 \\ 0 & 3.59 \cdot 10^{-13} & 0 \\ 0 & 0 & 3.59 \cdot 10^{-13} \end{bmatrix} \text{m}^2$$

$$\bar{K}_{tows,warp} = \begin{bmatrix} 7.68 \cdot 10^{-13} & 0 & 0 \\ 0 & 3.69 \cdot 10^{-12} & 0 \\ 0 & 0 & 7.68 \cdot 10^{-13} \end{bmatrix} \text{m}^2$$

Unsaturated flow simulation

- Boundary conditions :

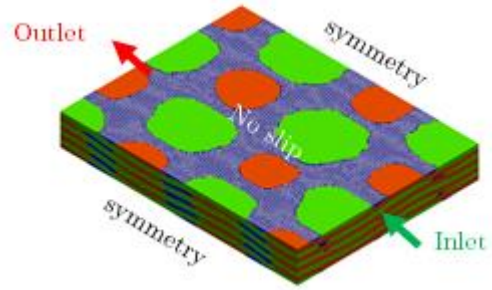

- 41*71*53 = 154283 elements
- Calculated for 200 seconds of filling
  - $Co = \frac{|\bar{u}|\delta t}{\delta l} < 0.05$

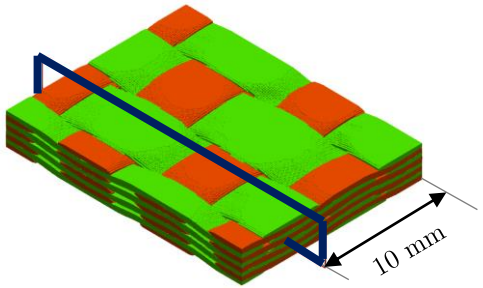

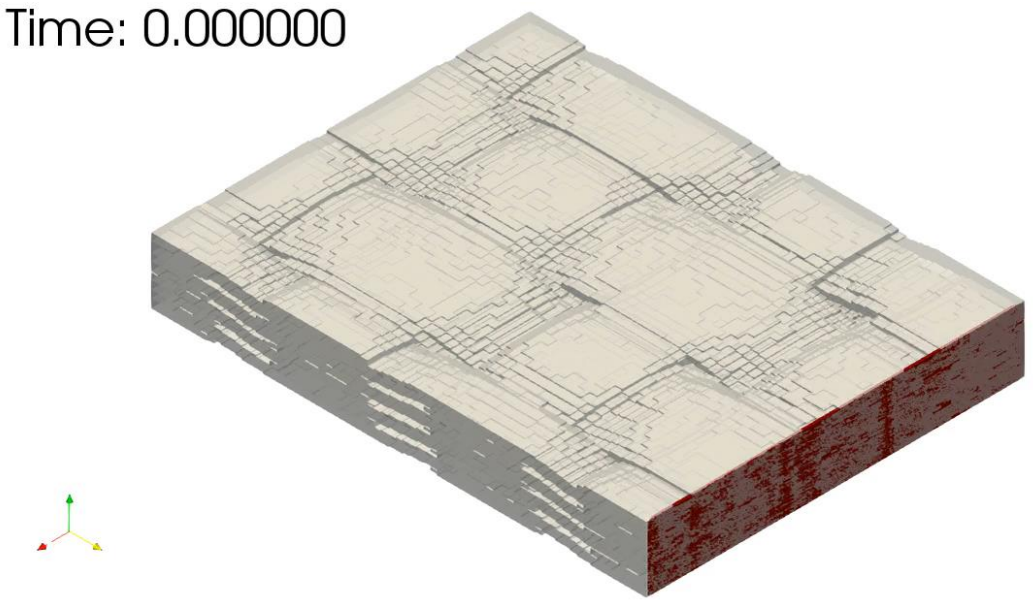

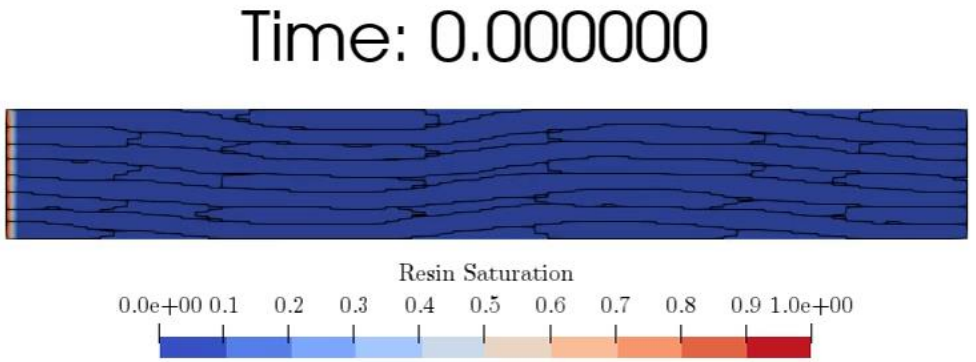

Synthesis characterization

W. Han, Q. Govignon, A. Cantarel, F. Schmidt (2022)
W. Han (2022)

C. Vicard (2018)
C. Vicard, O. De Almeida, A. Cantarel, and G. Bernhart. (2019)

Heat flow from PA6 synthesis DSC

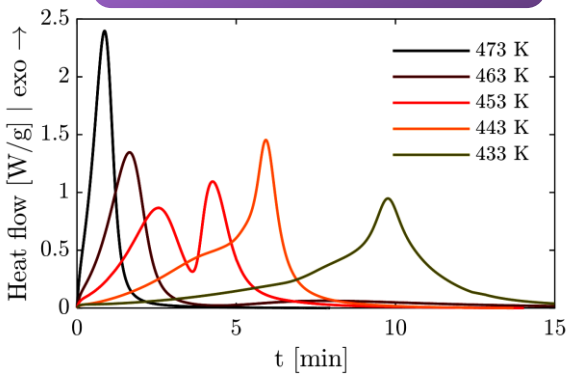

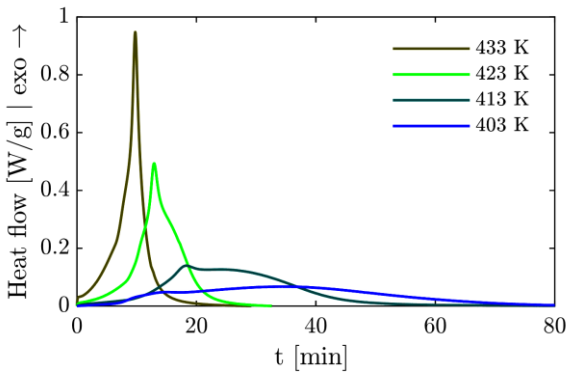

Polymerization model

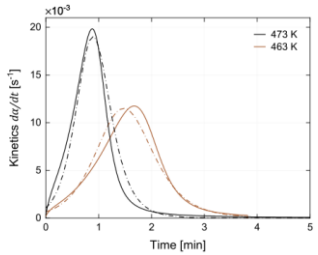

- Malkin and Camargo model

$$\dot{a}(a) = A_1 \exp\left(-\frac{E_{a,1}}{RT}\right)(1-a)^{n_p}(1+B_0 a)$$

Crystallization model

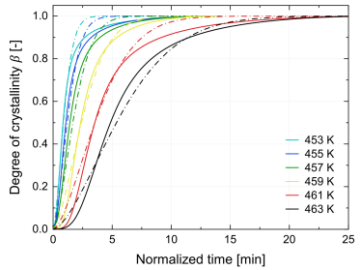

- Nakamura-Hoffman-Lauritzen model

$$\dot{b}(t) = a_a K_c\big(T(t)\big)(1-\beta) n_c \ln\left(\frac{1}{1-\beta}\right)^{\frac{n_c-1}{n_c}}$$

Synthesis characterization

W. Han, Q. Govignon, A. Cantarel, F. Schmidt (2022)
W. Han (2022)

C. Vicard (2018)
C. Vicard, O. De Almeida, A. Cantarel, and G. Bernhart. (2019)

Heat flow from PA6 synthesis DSC

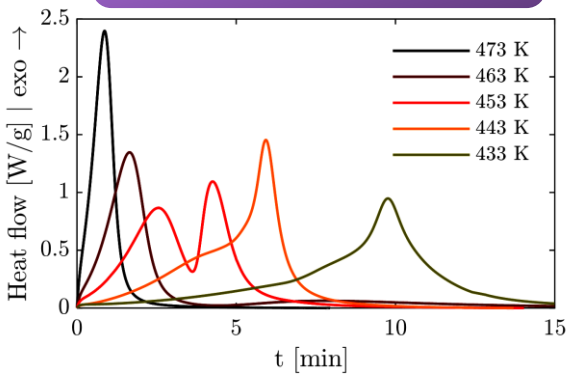

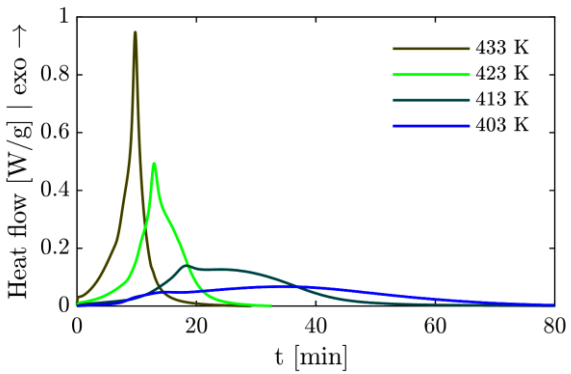

Polymerization model

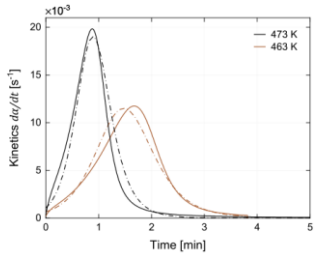

- Malkin and Camargo model

$$\dot{a}(a) = A_1 \exp\left(-\frac{E_{a,1}}{RT}\right)(1-a)^{n_p}(1+B_0 a)$$

Crystallization model

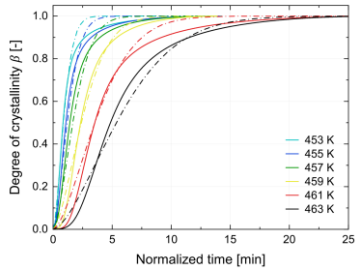

- Nakamura-Hoffman-Lauritzen model

$$\dot{b}(t) = a_a K_c\big(T(t)\big)(1-\beta) n_c \ln\left(\frac{1}{1-\beta}\right)^{\frac{n_c-1}{n_c}}$$

Heat flow modelling

$$\varphi_s(t) = \varphi_p(a) + \varphi_c(b)$$

a : polymerization degree
b : crystallization degree

- Coupled crystallization - polymerization method

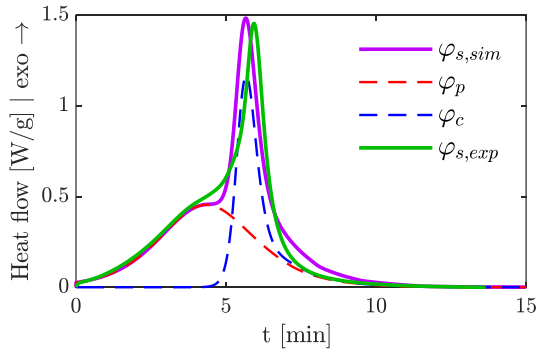

Synthesis characterization

W. Han, Q. Govignon, A. Cantarel, F. Schmidt (2022)
W. Han (2022)

C. Vicard (2018)
C. Vicard, O. De Almeida, A. Cantarel, and G. Bernhart. (2019)

Heat flow from PA6 synthesis DSC

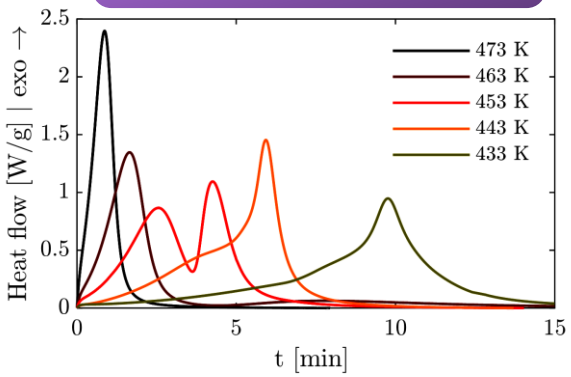

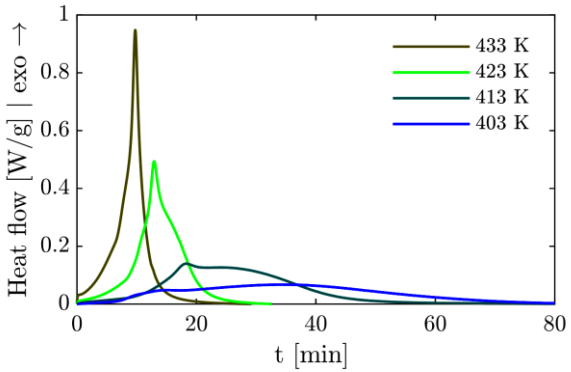

Polymerization model

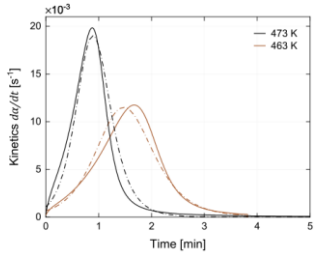

- Malkin and Camargo model

Crystallization model

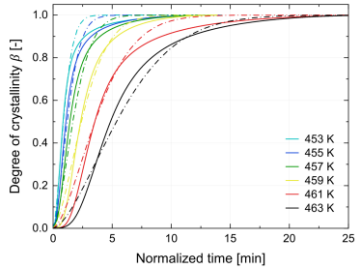

- Nakamura-Hoffman-Lauritzen model

Rheokinetics

$$\eta(T, a, b) = \eta_{r,0}(T)\exp\left(K_{\eta,a}X_a\right)\exp\left(K_{\eta,b}{X_c}^2\right)$$

170°C

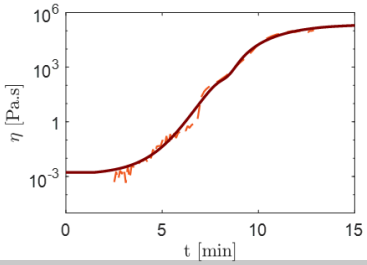

Rheological measurements

Parallel plate rheometry

- *Anton Paar MCR302 (picture) (TPCIM, IMT Nord Europe – Douai)*
- *Thermo Scientific™ HAAKE™ MARS™ 60 (Thermo Fisher Scientific – Courtaboeuf)*

Injection simulation principle

Anisothermal simulation

- **Incompressible heat equation**

$$\bar{\rho}\bar{c_p}\frac{\partial T}{\partial t} + \rho c_p \nabla \cdot (\boldsymbol{u}T) - \nabla \cdot (\bar{\kappa}\nabla T) = \dot{q}_s$$

  - Mix law for $\bar{\kappa}$, $\bar{\rho}$, $\bar{c_p}$,
  - ρ, c_p are resin properties

- $\dot{q}_s = \frac{\varphi_s \alpha_{resin}}{c_{p,resin}}$ **heat source term from synthesis exothermy**

$$\alpha_{resin} = \tilde{\varepsilon} S_1$$

  - $\varphi_s(t) = \varphi_p(a,t) + \varphi_c(b,t)$

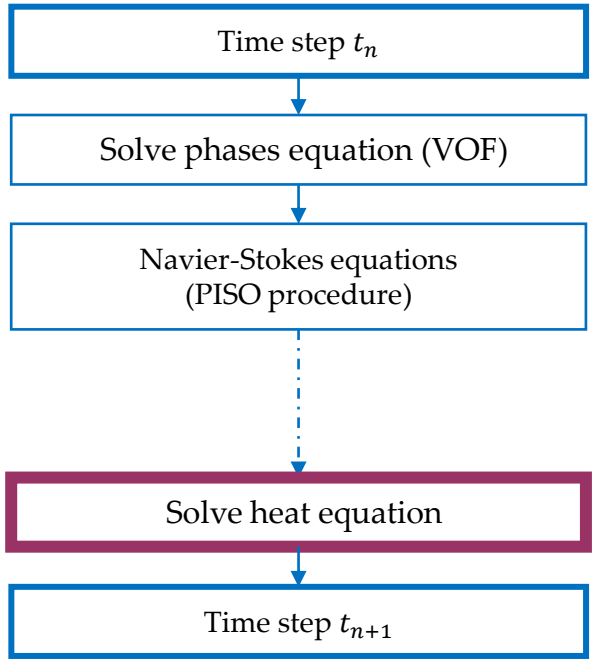

Injection simulation principle

Anisothermal simulation

- **Incompressible heat equation**

$$\bar{\rho}\bar{c_p}\frac{\partial T}{\partial t} + \rho c_p \nabla \cdot (\boldsymbol{u}T) - \nabla \cdot (\bar{\kappa}\nabla T) = \dot{q}_s$$

  - Mix law for $\bar{\kappa}$, $\bar{\rho}$, $\bar{c_p}$,
  - ρ, c_p are resin properties

- $\dot{q}_s = \frac{\varphi_s \alpha_{resin}}{c_{p,resin}}$ **heat source term from synthesis exothermy**

$$\alpha_{resin} = \tilde{\varepsilon} S_1$$

  - $\varphi_s(t) = \varphi_p(a,t) + \varphi_c(b,t)$

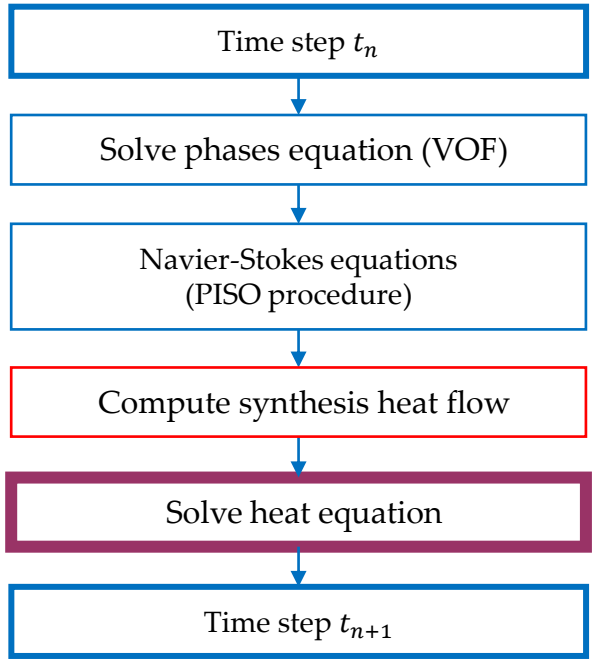

Injection simulation principle

Integration of polymerization calculation

- $\varphi_s(t) = \varphi_p(a,t) + \varphi_c(b,t)$

  $= \Delta H_p^{\infty} \dot{a}(a) + \Delta H_c^{\infty}(T) \dot{b}(T, b, a_a)$

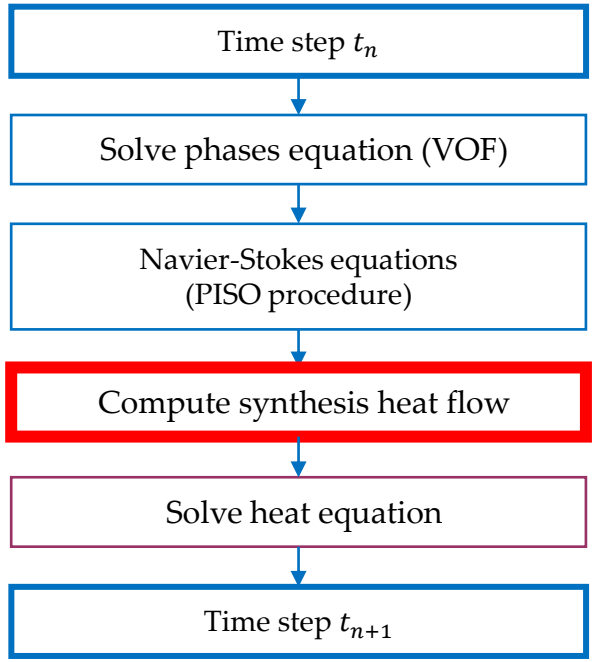

Injection simulation principle

Integration of polymerization calculation

- $\varphi_s(t) = \varphi_p(a,t) + \varphi_c(b,t)$

  $= \Delta H_p^\infty \dot{a}(a) + \Delta H_c^\infty(T)\dot{b}(T,b,a_a)$

- **Calculation of polymerization degree**

$$\frac{\partial a}{\partial t} + \boldsymbol{\nabla}\cdot(\boldsymbol{u}a) = \tilde{\varepsilon} S_r \dot{a}(a)$$

Polymerization transport equation (FVM discretization)

Polymerization rate (modified Malkin & Camargo)

$$\dot{a}(a) = A_1 \exp\left(-\frac{E_{a,1}}{RT}\right)(1-a_t)^{n_p}(1+B_0 a_t)$$

$$a_t = \frac{a}{\tilde{\varepsilon} S_r}$$

- a is the volume-averaged polymerization degree
- a_t is the true polymerization degree

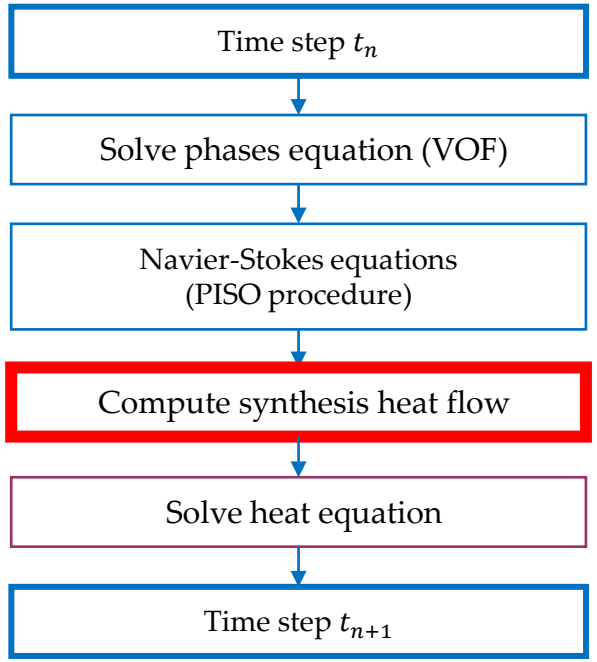

Injection simulation principle

Integration of crystallization calculation

- $\varphi_s(t) = \varphi_p(a,t) + \varphi_c(b,t)$

  $= \Delta H_p^\infty \dot{a}(a) + \Delta H_c^\infty(T)\dot{b}(T,b,a_a)$

  - Anisothermal crystallization is tracked using crystallization enthalpy $\Delta H_c(t) = b(t)\Delta H_c^\infty(T)$
  - Crystallization degree is calculated following a Nakamura model coupled with polymerization

    W. Han, Q. Govignon, A. Cantarel, F. Schmidt (2022)

    $$\dot{b}(t) = a_a K_c\big(T(t)\big)(1-\beta)n_c \ln\left(\frac{1}{1-\beta}\right)^{\frac{n_c-1}{n_c}}$$

    $$\beta = \frac{b}{a_a(a_t, t_{c,0})}$$

    - a_a : Polymer availability
    - β : Local crystallization degree
  - Transport equation are used to calculate relevant scalar fields

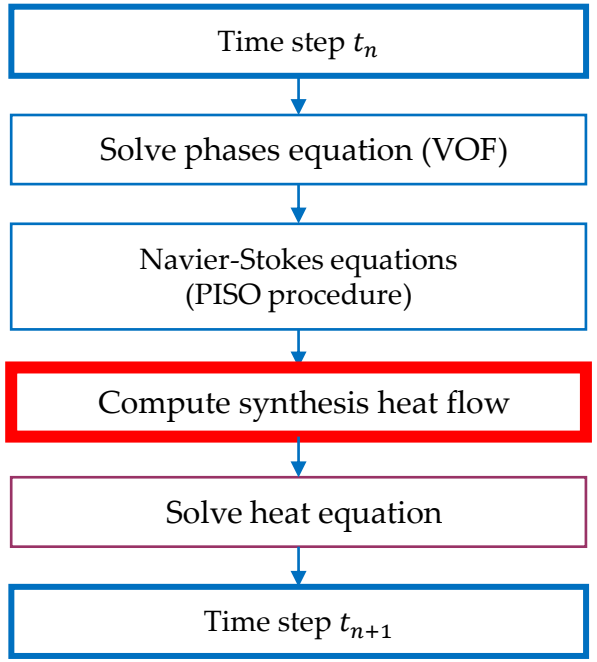

Boundary conditions

- Top side :
  - No slip (U=0)
  - Fields : zero gradient ($\frac{\partial \phi}{\partial n} = 0$)
  - $\frac{\partial T}{\partial n} = 0$
- Bottom side
  - No slip (U=0)
  - Fields : zero gradient ($\frac{\partial \phi}{\partial n} = 0$)
  - T = 433 K
- 20*71*53 = 75260 elements
- Calculated for 200 seconds of filling
  - $Co = \frac{|\bar{u}|\delta t}{\delta l} < 0.05$

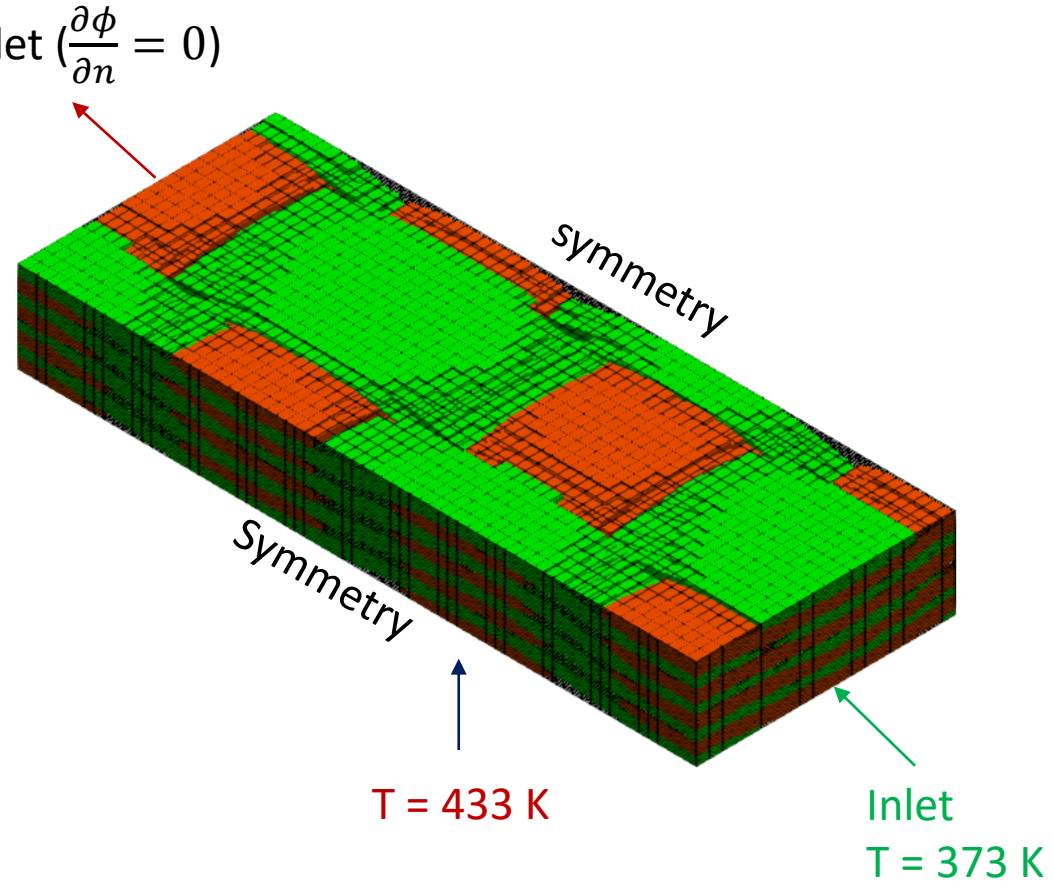

Reactive injection simulation

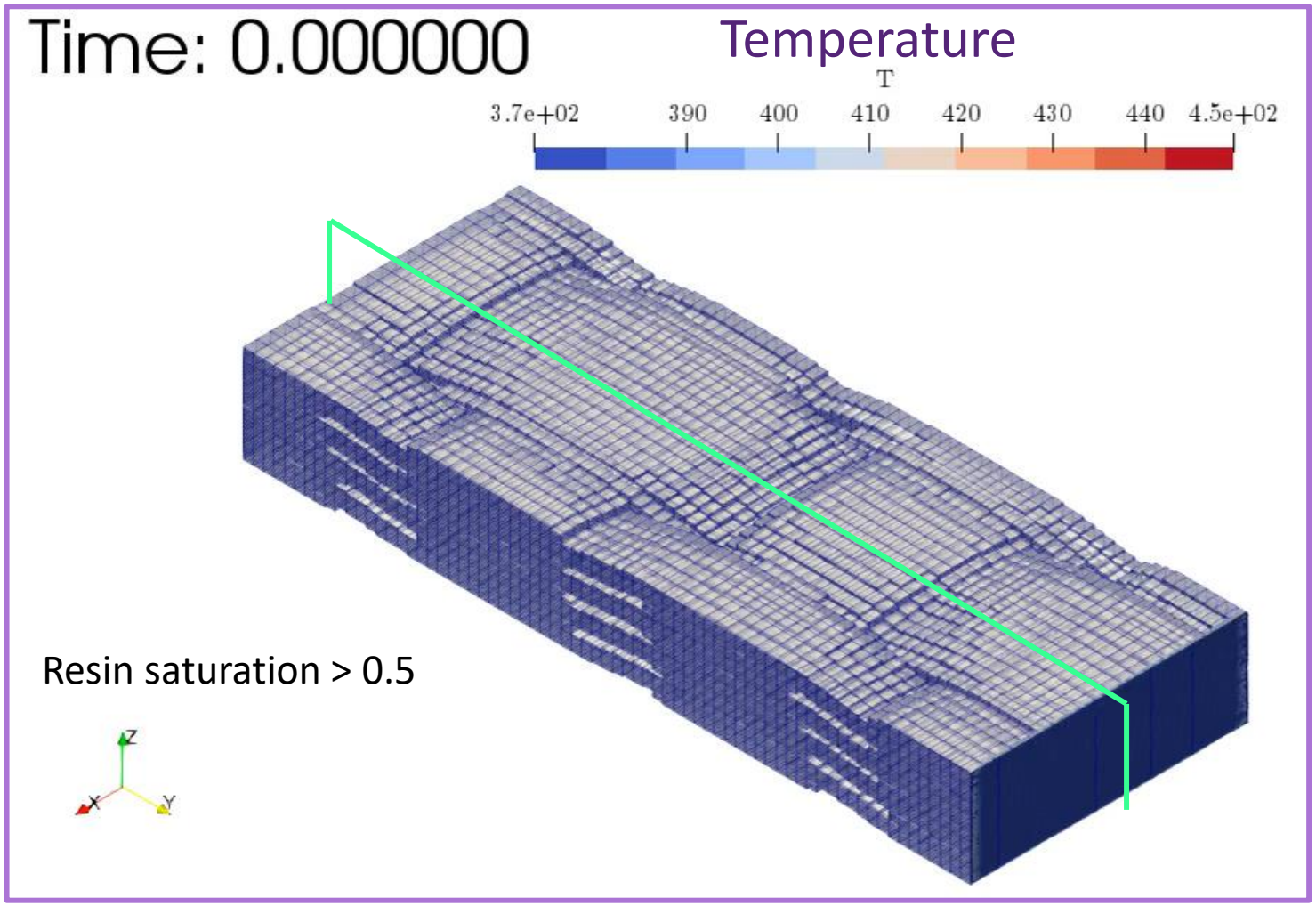

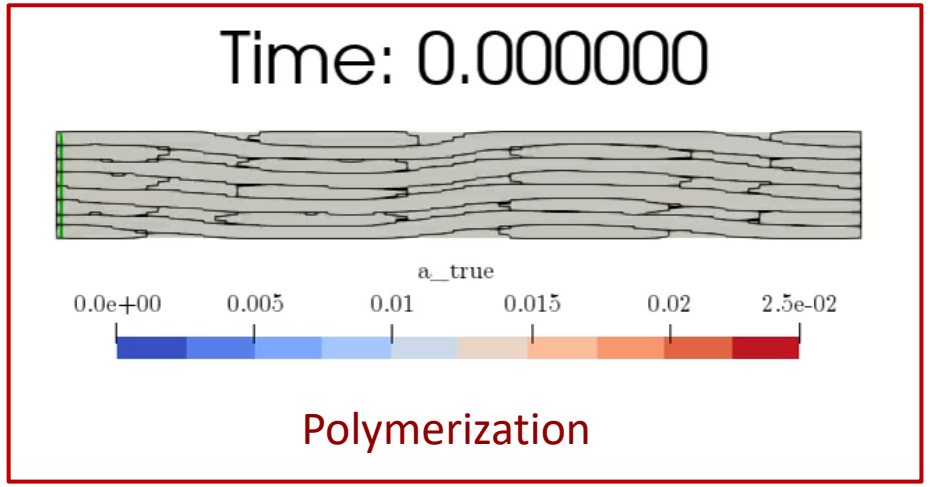

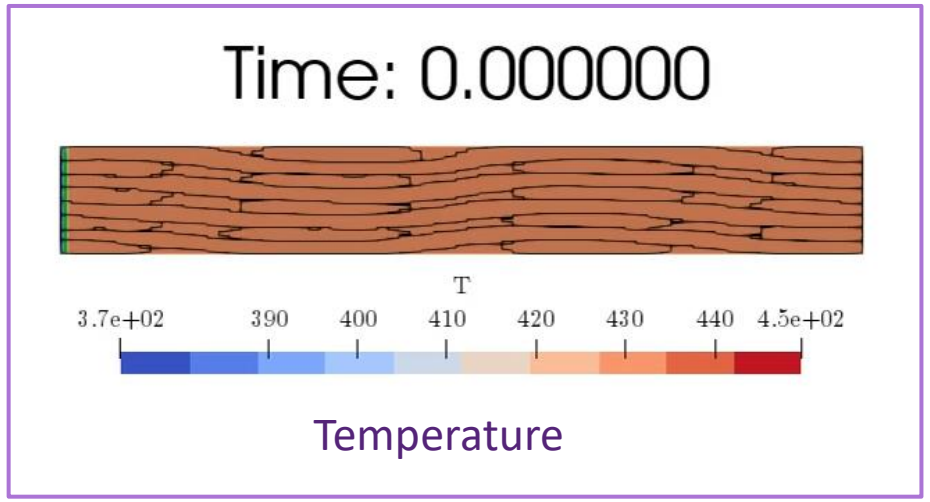

Reactive injection simulation

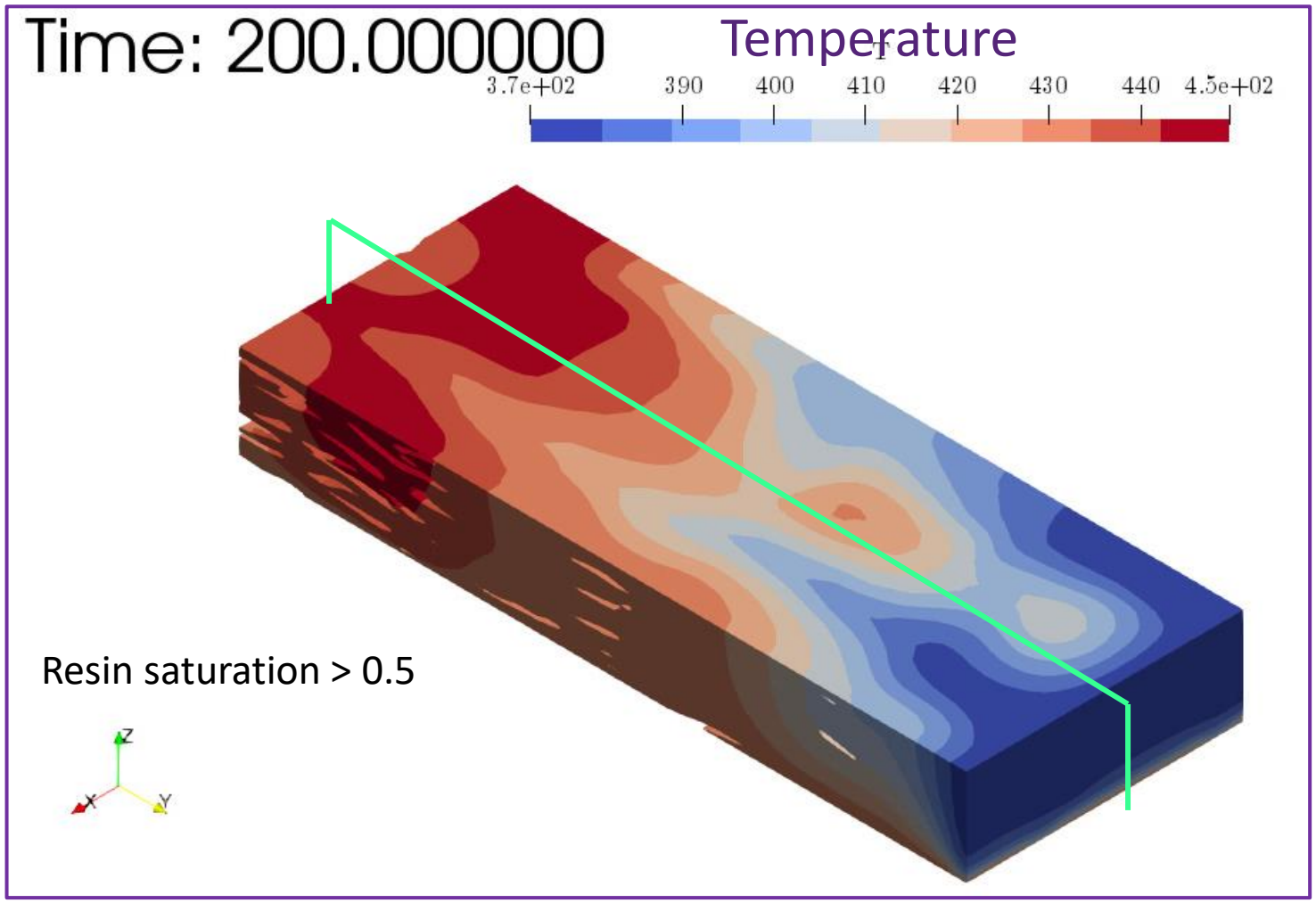

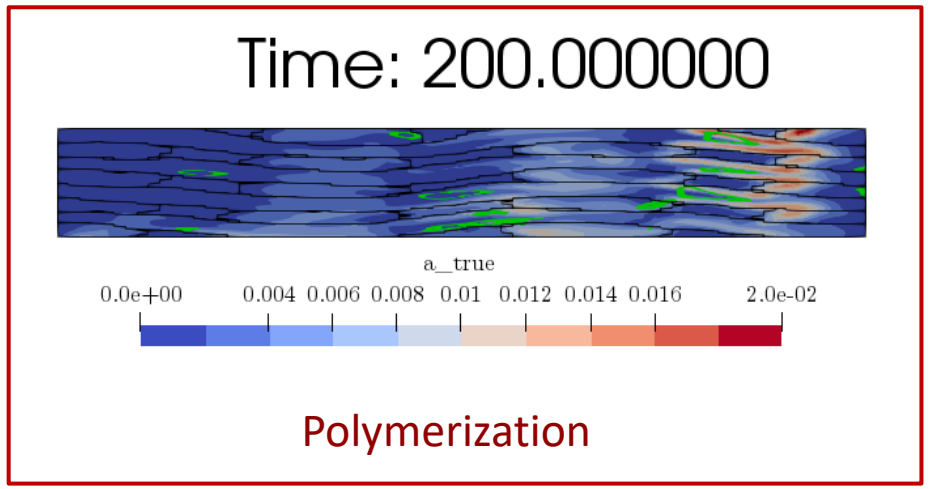

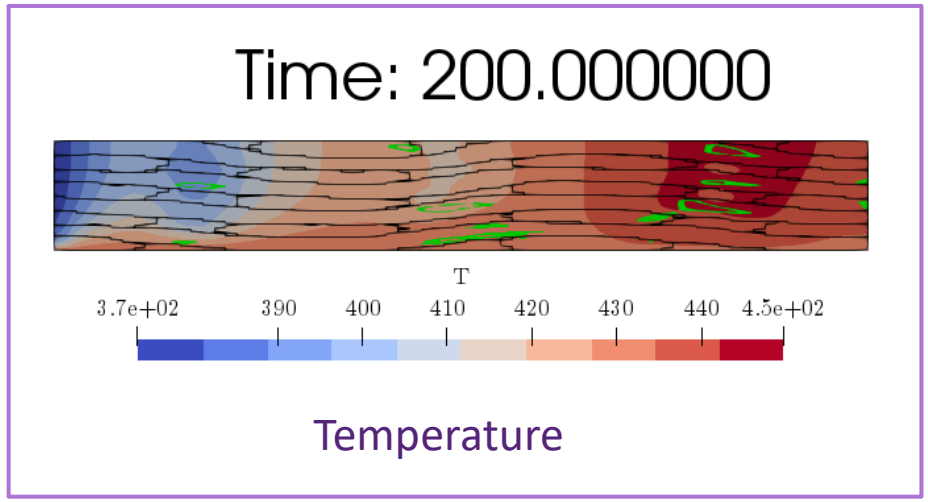

Synthesis simulation after injection

Pressure, velocity, saturation are not solved

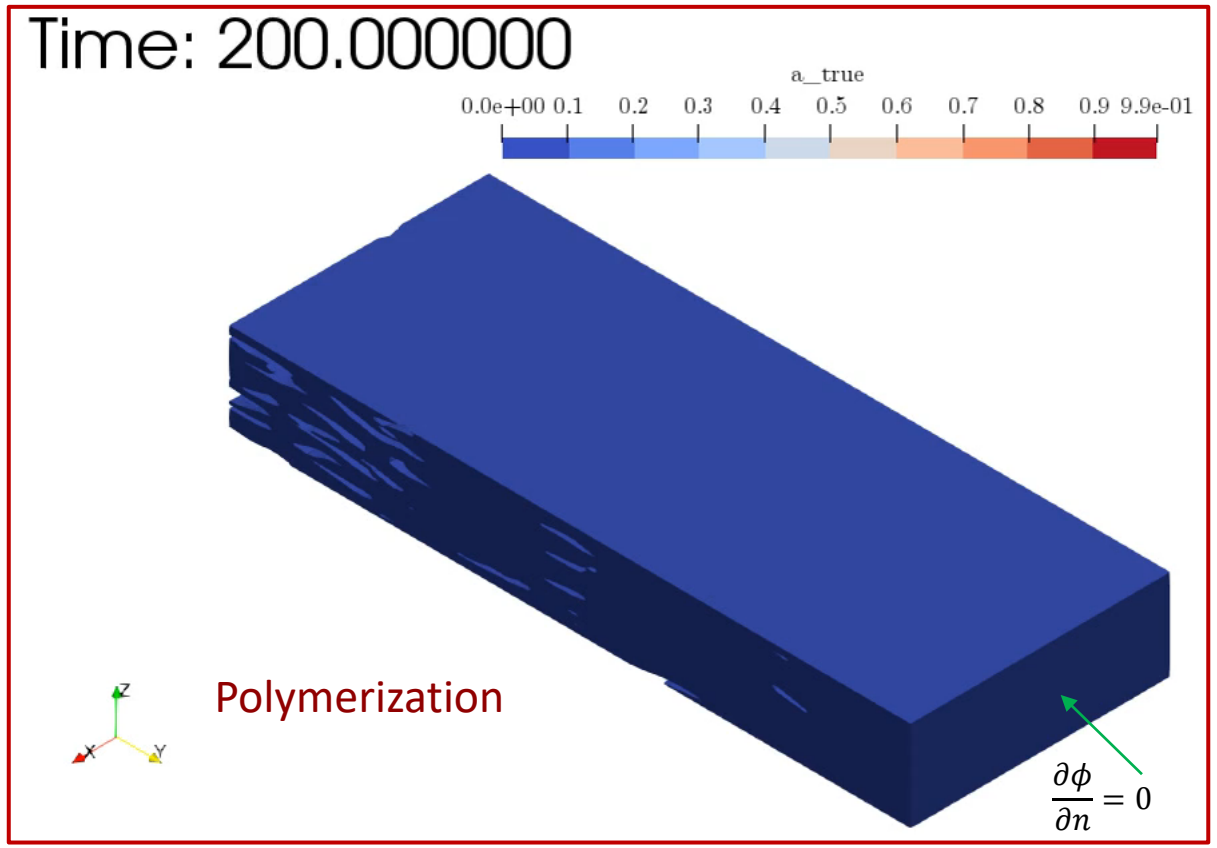

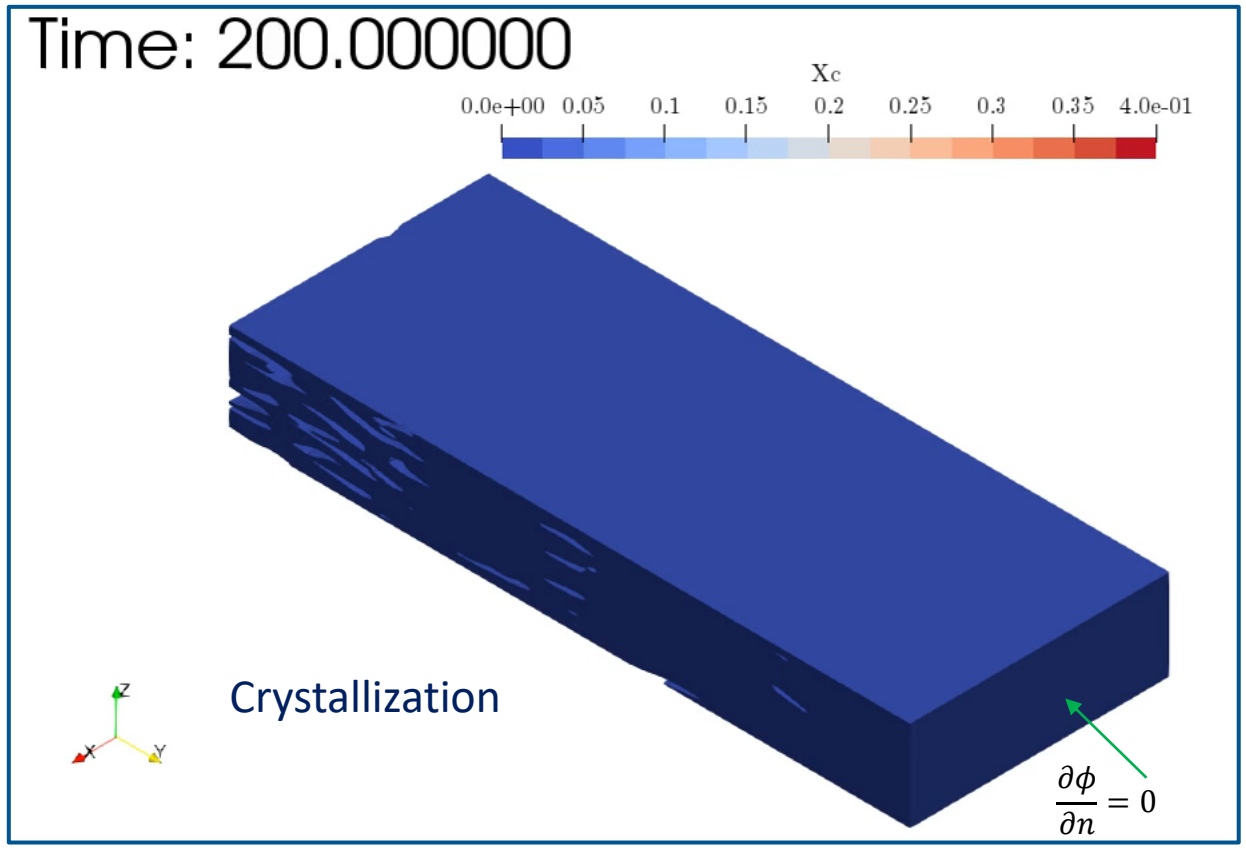

Resin saturation > 0.5

Synthesis simulation after injection

Pressure, velocity, saturation are not solved

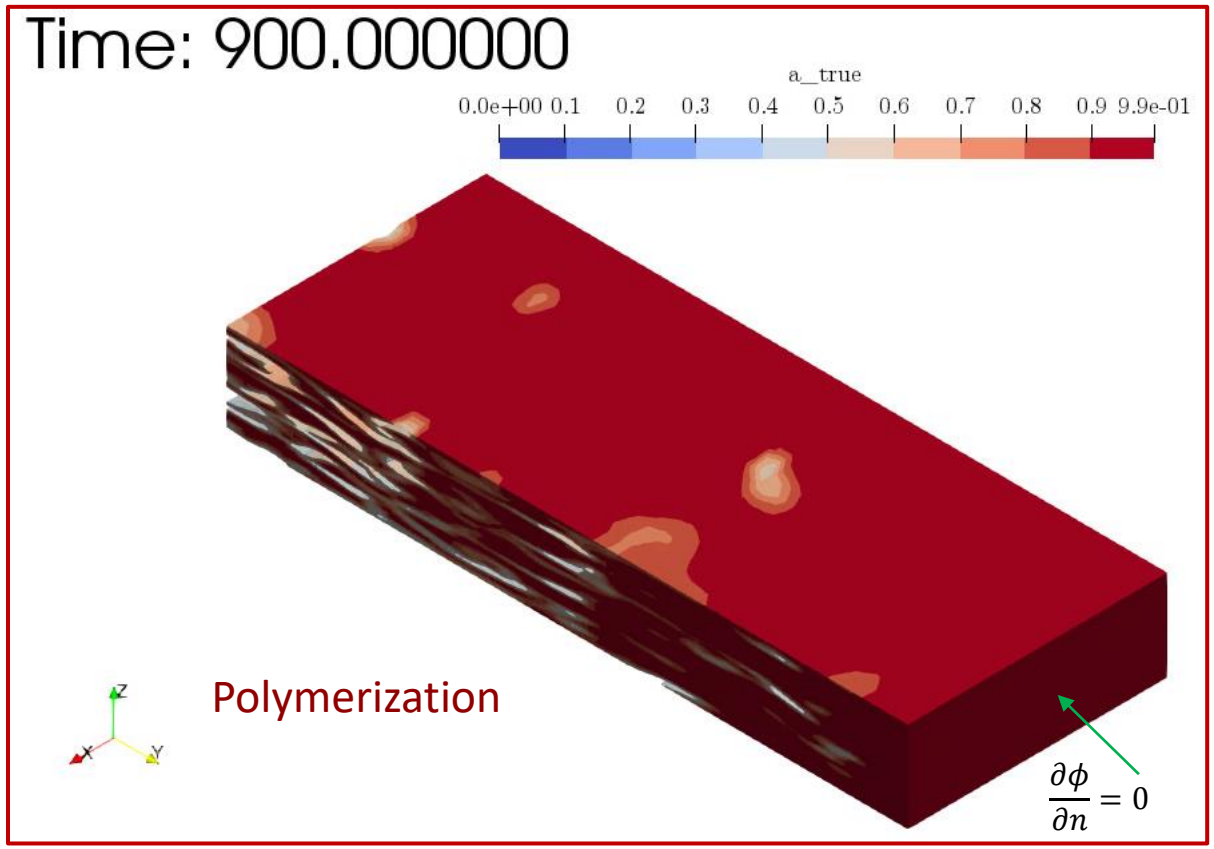

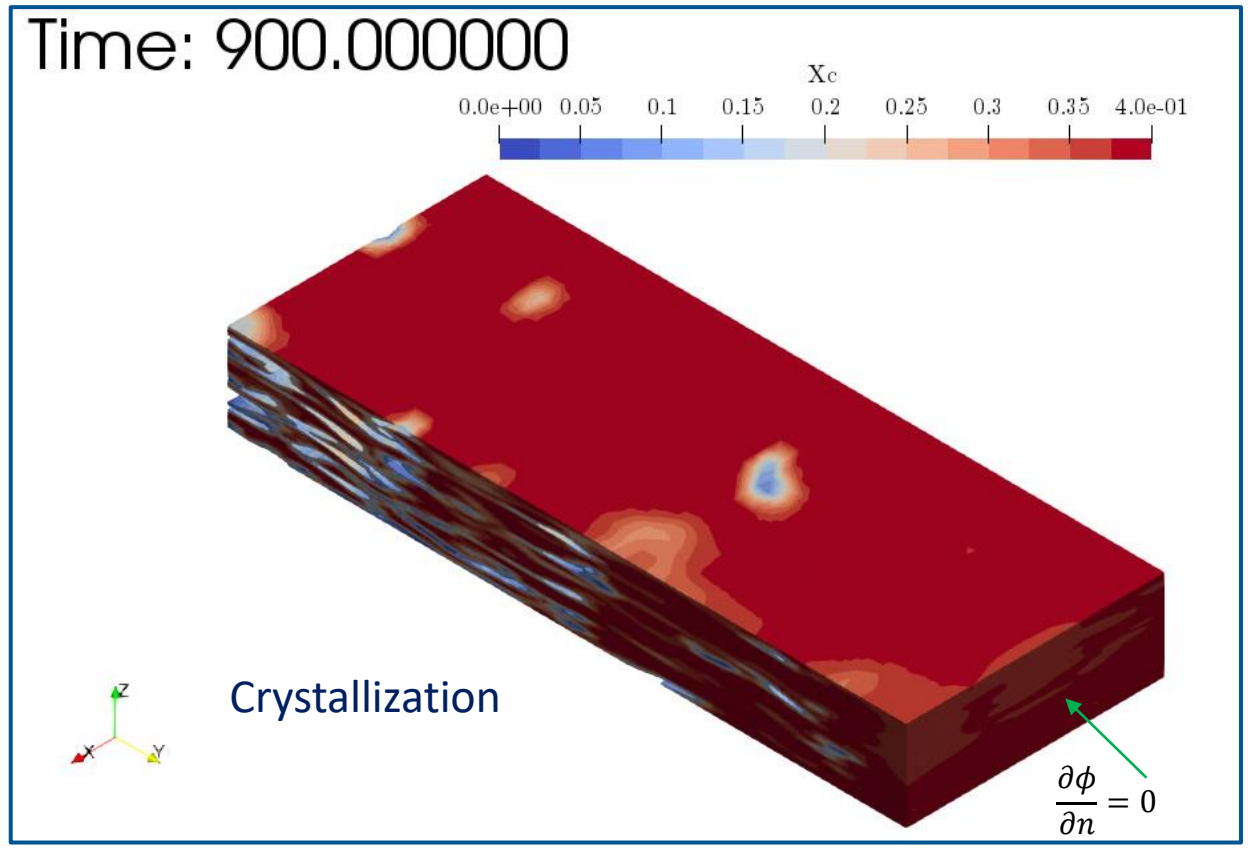

Resin saturation > 0.5

Conclusion and perspectives

Study of resin flow simulation

- Integration of synthesis model for a reactive anisothermal flow simulation
- Realistic textile geometry flow simulation using Navier-Stokes-Brinkman equation

Perspectives

- Flow interaction with fibre preform
  - Study surface tension of reactive mix and integrate capillary effects
  - Study tow geometry influence
- Experimental reactive mix injection
  - Instrumented composite manufacturing
- Process optimization using numerical simulations

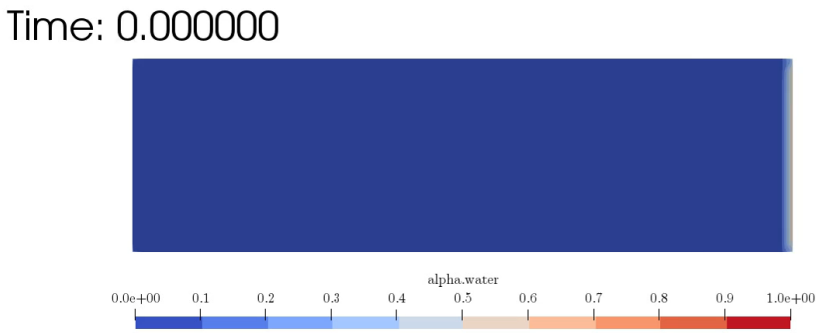

INSTITUT CLÉMENT ADER

La Région Occitanie Pyrénées - Méditerranée

Thank you for your attention

ICCM 23 INTERNATIONAL CONFERENCE ON COMPOSITE MATERIALS BELFAST 2023 30 JULY – 4 AUGUST

IMT Mines Albi-Carmaux École Mines-Télécom · INSA Institut National des Sciences Appliquées Toulouse · isae Institut Supérieur de l'Aéronautique et de l'Espace SUPAERO · Université Toulouse III Paul Sabatier · cnrs · Université Fédérale Toulouse Midi-Pyrénées